Quaternary Science Reviews 45 (2012) 73–84

Contents lists available at SciVerse ScienceDirect

Quaternary Science Reviews

journal homepage: www.elsevier.com/locate/quascirev

ITCZ and ENSO-like pacing of Nile delta hydro-geomorphology during the Holocene

Nick Marriner [a,*], Clément Flaux [b], David Kaniewski [c], Christophe Morhange [b], Guillaume Leduc [d], Vincent Moron [b,e], Zhongyuan Chen [f], Françoise Gasse [a], Jean-Yves Empereur [g], Jean-Daniel Stanley [h]

[a] CNRS, CEREGE UMR 7330, Europôle de l'Arbois, BP 80, 13545 Aix-en-Provence Cedex 04, France
[b] Université Aix-Marseille, CEREGE UMR 7330, Europôle de l'Arbois, BP 80, 13545 Aix-en-Provence Cedex 04, France
[c] Université Paul Sabatier-Toulouse 3, EcoLab (Laboratoire d'Ecologie Fonctionnelle), Bât 4R1, 118 Route de Narbonne, 31062 Toulouse cedex 9, France
[d] Universität Kiel, Earth Science Institute, Ludewig-Meyn-Str. 10, D-24118 Kiel, Germany
[e] International Research Institute for Climate and Society, Columbia University, New York, NY, USA
[f] East China Normal University, Shanghai 200062, China
[g] Centre d'Études Alexandrines, CNRS, UMS 1812, 50 rue Soliman Yousri, 21131 Alexandria, Egypt
[h] Geoarchaeology Program, Rm. E-205, National Museum of Natural History (NMNH), Smithsonian Institution, Washington, D.C. 20013-7012, USA

ARTICLE INFO

Article history:
Received 5 September 2011
Received in revised form
26 March 2012
Accepted 25 April 2012
Available online xxx

Keywords:
Nile
Delta
Holocene climate change
ITCZ
ENSO
Civilizations

ABSTRACT

The Nile valley accommodates the world's longest river and shaped the development of numerous complex societies, providing a reliable source of water for farming and linking populations to sub-Saharan Africa and the Mediterranean Sea. Its fertile delta lay at the heart of ancient Egyptian civilization, however little is known of its morpho-sedimentary response to basin-wide changes in Holocene hydrology. Here, we present two well-resolved records from the Nile delta (based on ~320 radiocarbon dates) to reconstruct the timing and rhythm of catchment-scale modifications during the past 8000 years. On the orbital timescale, we demonstrate that Nilotic hydrology and sedimentation have responded to low-latitude insolation forcing while, on sub-millennial timescales, many of the major phases of deltaic modification were mediated by climate events linked to El Niño Southern Oscillation-type (ENSO) variability.

1. Introduction

Continental rivers and their mega-deltas constitute rich archives of Holocene change and human activities (Törnqvist, 1994; Krom et al., 2002). Within this context, the Nile delta is ideally suited to record variations in East African hydrological balance and anthropogenic forcings owing to its assimilation of basin-scale (~3,350,000 km^2) changes from a wide latitudinal range, spanning the equatorial zone (4°S) to the Mediterranean (31°N) (Woodward et al., 2007). Although it has a well-investigated late Quaternary record (Stanley and Warne, 1993; Stanley et al., 1996), its response to catchment-wide climatic fluctuations and human impacts is unclear. To fill this knowledge gap, we constructed two high-resolution and regional-scale time-series, based on 105 evenly distributed sediment cores and sections studded across the deltaic plain (Fig. 1a). Because of its geographical location, and links to other climate zones of the world, the Nile valley is a key region to study the possible global nature of climate variability and its role in driving societal change (Butzer, 1976; Welsby et al., 2002; Nicoll, 2004; Brooks, 2006, 2011; Kuper and Kröpelin, 2006; Staubwasser and Weiss, 2006). In effect, changes in the Nile's Holocene palaeohydrology have significantly impacted upon the nature and distribution of human activity along its fluvial corridor and bordering regions (Woodward et al., 2001).

In sub-equatorial and tropical regions of Africa, one process frequently invoked to explain Holocene changes in precipitation and hence hydrology is a shift in the dynamics of the Intertropical Convergence Zone (ITCZ), which migrates latitudinally in response to orbitally-controlled climatic processes (Fig. 1b). While this mechanism is well attested in regional archives, including ice-cores (Thompson et al., 2002), lacustrine records (Roberts and Barker, 1993; Gasse, 2000; Kröpelin et al., 2008; Verschuren et al., 2009) and marine sediments (Ducassou et al., 2008; Revel et al., 2010), few studies have focused on the Nile delta as a regional-scale palaeoclimate archive.

* Corresponding author.
E-mail address: marriner@cerege.fr (N. Marriner).

0277-3791/$ – see front matter © 2012 Elsevier Ltd. All rights reserved.
doi:10.1016/j.quascirev.2012.04.022

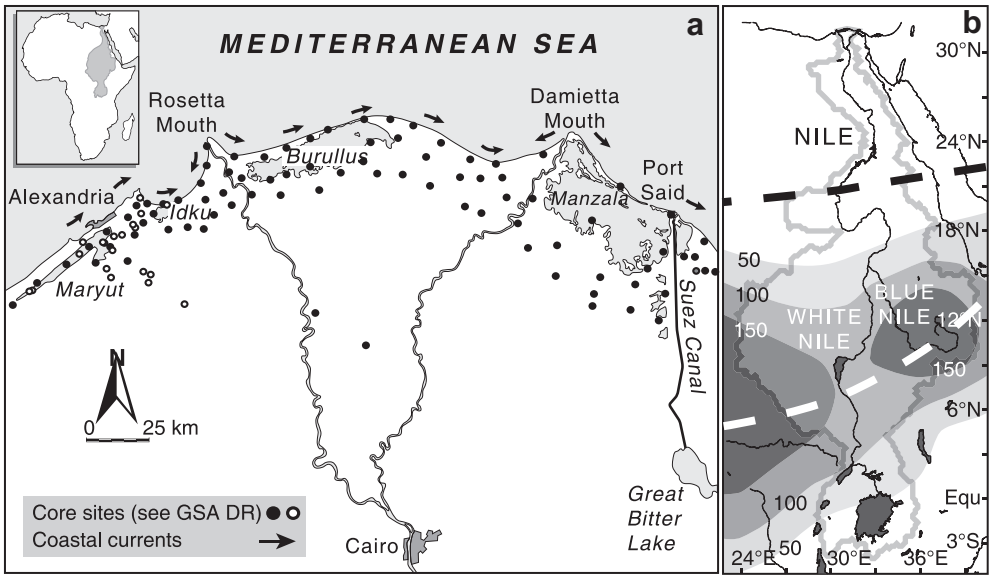

Fig. 1. Location maps. (a) Position of radiocarbon dated cores/sections ($n = 105$) used in this study. (b) The Nile catchment. Black dotted line denotes the approximate position of the June–July–August ITCZ during the Holocene monsoonal maximum (Gasse, 2000); white dotted line denotes the present position of the JJA ITCZ. Circles denote core sites (grey circles (Sneh et al., 1986), black circles (Stanley and Warne, 1993; Stanley et al., 1996, 2008) and white circles (Flaux et al., 2011; Flaux, 2012)).

Recently, laminated lake sediments from eastern equatorial Africa have been used to reconstruct interannual rainfall changes which are nowadays linked to El Niño Southern Oscillation (ENSO) activity in this region (Wolff et al., 2011). Lower interannual rainfall variability is attested during the Last Glacial Maximum, reflecting reduced ENSO activity as reported for marine sediments collected in the equatorial Pacific (Leduc et al., 2009). These results suggest that past rainfall changes in the Nile catchment were also sensitive to ENSO, which is known to have varied at the sub-millennial timescale during the Holocene (Moy et al., 2002; Marchitto et al., 2010). In this paper, our aim is to explore regional-scale Nile delta changes, operating at orbital and sub-millennial timescales, using deltaic chronostratigraphy.

2. Methods

2.1. Nile delta database

We compiled a database of radiocarbon dates from the Nile delta using various literature sources (Sneh et al., 1986; Stanley and Warne, 1993; Stanley et al., 1993, 2008) and our present ongoing research (around 100 new cores/sections and 49 unpublished radiocarbon dates; Flaux et al., 2011; Flaux, 2012). The radiocarbon dates incorporated into the database derive from reliable sedimentary logs in peer-reviewed publications. We focused our attention on the last 8000 years, as this time period corresponds to the morphogenesis of the present delta system (Stanley and Warne, 1993). The large size of this base-level database enables us to assimilate many tributary signals from the Nile catchment, which may arrive diachronously from distant source areas. Traditionally, this has hindered the interpretation of downstream stratigraphic records in continental rivers (see Törnqvist, 1994 for an exception to this). To standardise the different data sources we structured results into 25 tabular fields, including information on geographic location, dated material, facies type and stratigraphic context. Particular attention was paid to facies change dates, representing a transition in the depositional context. The robustness of this technique in reconciling regional-scale fluvial changes during the Holocene has been highlighted by a rich literature with a particular focus on the UK (Macklin et al., 2010) and Europe (Macklin et al., 2006). Dates from archaeological contexts were excluded in order to reduce bias linked to human occupation of the floodplain. A total of 359 entries were made in the database; 41 dates were judged to have been reworked and were excluded from subsequent analyses. Facies change dates totalled 202 entries. Locations of core sites and sections ($n = 105$) are given in Fig. 1a.

2.2. Nile delta sedimentation rates

Spatially averaged sedimentation rates were calculated for all radiocarbon couplets. A matrix in annual increments was plotted for all minimum ($n = 258$) and maximum ($n = 258$) sedimentation pairs to generate upper and lower boundaries. We subsequently summed annual increments and divided by the population present in each year to generate a spatially averaged sedimentation figure for the whole delta area. Sedimentation rates were pooled ($n = 516$) to produce the mid-range curve. All rates were summed in 100-year non-overlapping windows to generate the final time-series in century^{-1}.

2.3. Cumulative probability plots

To standardise all radiocarbon dates, determinations were calibrated and summed using Oxcal (Bronk Ramsey, 2000) with the IntCal09 and Marine09 datasets (Reimer et al., 2009). All calibrations are quoted at the two-sigma confidence range. We used the cumulative probability option in Oxcal to analyse the data sub-sets (Fig. 2). Cumulative PDFs have been widely used to synthesize large radiocarbon datasets in fluvial geomorphology (Macklin and Lewin, 2003; Macklin et al., 2006, 2010; Thorndycraft and Benito, 2006) and archaeology (Kuper and Kröpelin, 2006; Turney and Hobbs, 2006; Bubenzer and Riemer, 2007), where probability peaks are respectively taken to be representative of hydrogeomorphological change and human occupation. The plots greatly facilitate comparison of datasets from diverse geographical and chronostratigraphic contexts, and the technique is therefore ideally suited to the Nile delta's substantial chronostratigraphic database.

To explore the large dataset, sub-sets of radiocarbon dates were systematically analysed, for example the facies change dates (Macklin et al., 2006, 2010) and types of depositional environment

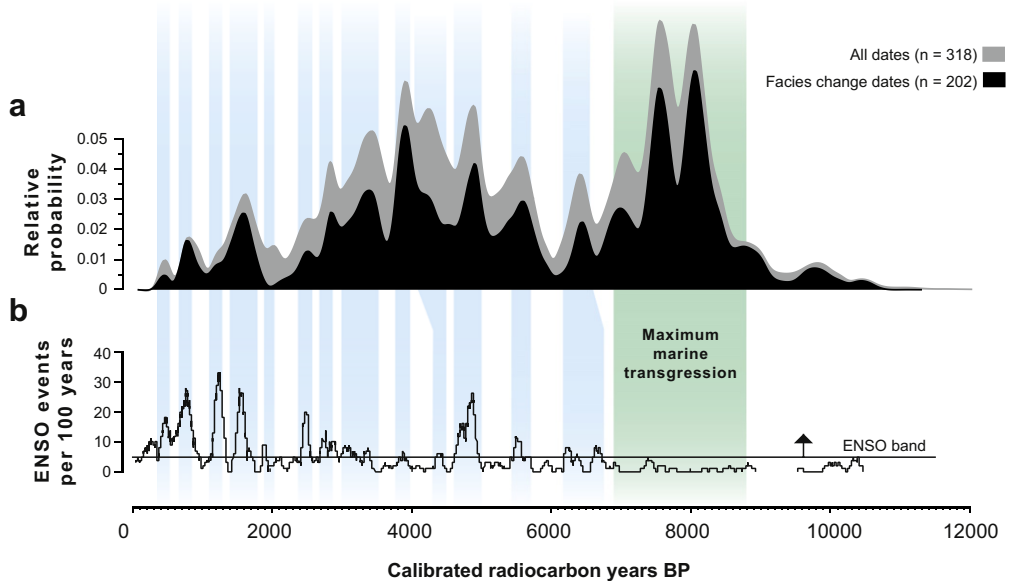

Fig. 2. (a) Summed PDF plots for radiocarbon dates from the Nile delta's Holocene record. The plot is divided into total dates and facies change dates for the period 12,000 cal. years BP to present. The *y*-axis is probability per year and the *x*-axis corresponds to the calibrated radiocarbon years BP (calibrated years before AD 1950). (b) The radiocarbon data are illustrated against the number of ENSO events per 100 years (Moy et al., 2002). The solid line denotes the minimum number of events in a 100-yr window needed to produce ENSO-band variance (~5). Periods of high ENSO-band variance are represented by the blue shading. (For interpretation of the references to colour in this figure legend, the reader is referred to the web version of this article.)

(Fig. 3). We paid particular attention to change dates as these are considered to be the best indicators in framing widespread catchment-scale modifications and downstream deltaic conditions (Macklin et al., 2010). These comprised facies shifts from one depositional environment to another, particularly a shift in the nature of alluviation or lagoon deposition driven by palaeohydrological changes. For the most part, three main categories were identified: marine ingression facies, progradation facies and avulsion facies. For instance, in the Maryut lagoon change dates essentially comprise a shift in sedimentation between two palaeoenvironmental contexts: a marine-influenced lagoon and a fluvial-influenced lagoon (Flaux, 2012; Fig. 4). After the Holocene marine transgression, these palaeoenvironmental 'oscillations' mirror palaeohydrological changes in Nile fluxes into the lagoon system. These changes have been reconstructed using core/section stratigraphy, biostratigraphy (malacology, micropalaeontology) and geochemistry (Sr and Pb isotopes). The results are fully outlined in Flaux (2012).

2.4. Statistical analyses

We used Cross-Correlation Analysis (CCA; $P = 0.05$) to compare and contrast our data with other proxy records (see below). Cross-Correlation Analysis (CCA; $P = 0.05$) is a generalization of detrended fluctuation analysis and is based on detrended covariance. CCA is a powerful tool in assessing the long-range cross-correlation between two non-stationary datasets (Podobnik and Stanley, 2008) and has produced robust results in hydrological studies (Hajiana and Sadegh Movahed, 2010). To quantify the power-law cross-correlations in non-stationary time-series (Nile, ENSO, Ethiopian Monsoon, Qunf Cave, Dongge Cave, Cariaco Basin), we have considered two long-range cross-correlated time-series of equal length. The cross-correlation is plotted as a function of alignment position. Positive correlation coefficients are considered, focussing on the Lag 0 value (with ca +0.50 as a significant threshold). Negative correlations are also assessed to test the inverse- or non-correlation between the two time-series (with ca −0.50 being a significant threshold). Null values indicate a complete absence of correlation. The ordination of palaeoclimatological archives was further tested using basic cluster analysis, principal components analysis, and non-metric multidimensional scaling for three periods (7000–4600, 4600–2500 and 2500–0 BP).

2.5. Comparison with palaeoclimatological archives

We compared and contrasted our data with a number of other palaeoclimatological archives. Records were normalized by averaging data into 100-year non-overlapping windows.

(a) *Egypt and Sudan Saharan archaeological data*. Archaeological radiocarbon data from the eastern desert of Egypt and Sudan were downloaded at: ftp://ftp.ncdc.noaa.gov/pub/data/paleo/radiocarbon. We recalibrated data in Oxcal and used the μ function to sort dates into non-overlapping 100-year windows. 825 dates were included in our analysis.

(b) *Lake Victoria (Pilkington Bay)* (Stager et al., 2003). Diatom data were downloaded at: ftp://ftp.ncdc.noaa.gov/pub/data/paleo/paleolimnology/eastafrica/victoria_pilkington_diatom.txt. CAST1 was derived using a Correspondence Analysis, Square root Transformed on the 36 most abundant diatom taxa in core 64-2 (Stager et al., 2003). The record is a proxy of lake depth. In Figs. 5b and 6, the scale has been inverted.

(c) *Qunf Cave, Oman* stalagmite record (Fleitmann et al., 2003, 2007). Raw data for plotting and statistical analyses were downloaded from the NOAA website at: http://www.ncdc.noaa.gov/paleo/metadata/noaa-cave-5541.html. $\delta^{18}O$ data were compared and contrasted with Nile sedimentation rates. Because of the inverse relationship between $\delta^{18}O$ and the amount of precipitation in regions affected by monsoons, $\delta^{18}O$ scales have been plotted high to low for comparative purposes with the Nile record.

(d) *Dongge Cave, China* stalagmite record (Wang et al., 2005). Raw data were retrieved at: http://www.ncdc.noaa.gov/paleo/metadata/noaa-cave-5439.html. See above.

(e) *Cariaco Basin*. Titanium and iron concentration data from the anoxic Cariaco Basin were used (Haug et al., 2001). Data were downloaded at: http://doi.pangaea.de/10.1594/PANGAEA.735654.

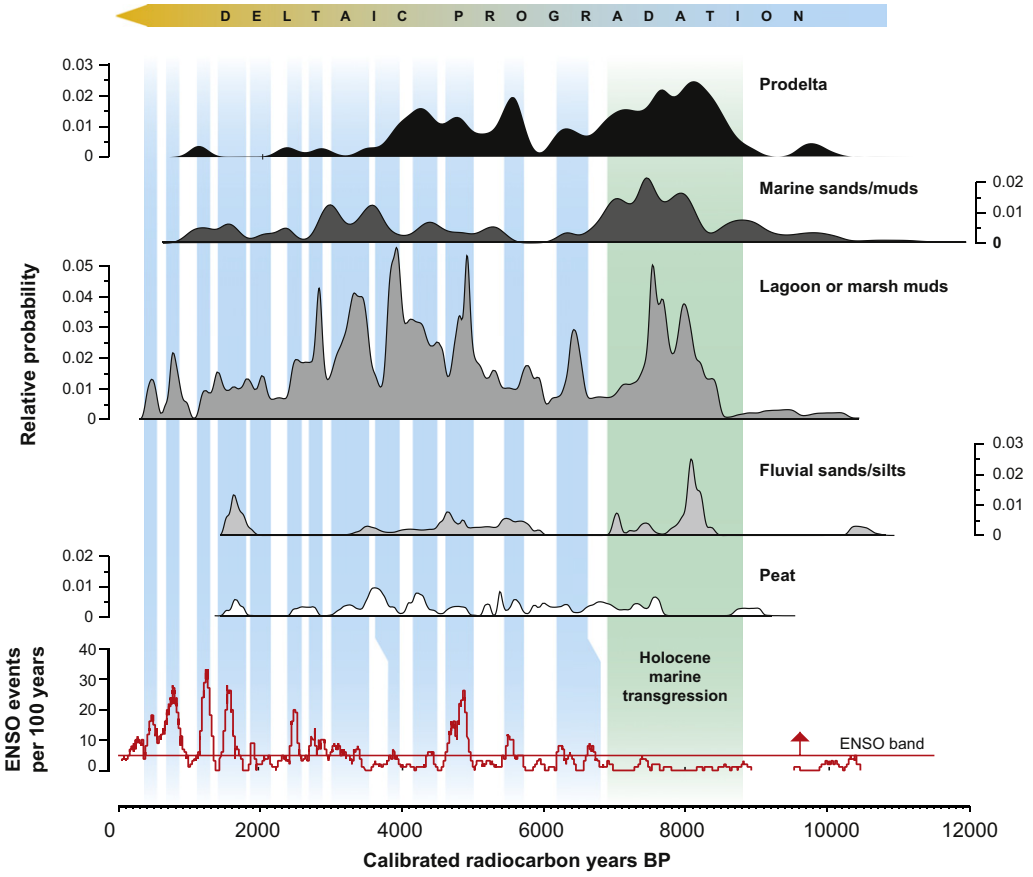

Fig. 3. Summed probability plots (0–12,000 cal. BP) structured into five dominant depositional environments: prodelta, marine sands/muds, lagoon marsh/muds, fluvial sands/silts and peats. The ENSO-like signal has been best recorded in low-energy lagoon or marsh muds. Deltaic progradation came in response to reduced base-level gradients and ponding (Butzer, 1997) when sea level stabilised ~6000 years ago.

(f) *Insolation*. Insolation quantities (W/m^2) in 100-year windows derived from the orbital and precessional quantities (Laskar et al., 2004) were downloaded at: http://www.imcce.fr/Equipes/ASD/insola/earth/online/index.php. Simulations were made for 10°N, 20°N and 30°N.

(g) *Laguna Pallcacocha, southern Ecuador ENSO record* (Moy et al., 2002). We compared the cumulative probability plots with Moy et al.'s high-resolution ENSO record from Laguna Pallcacocha, southern Ecuador, which spans the period 12,000 years to present. Raw data for plotting and analytical purposes were downloaded from the NOAA website at: http://www.ncdc.noaa.gov/paleo/pubs/moy2002/. By comparison with the Quinn El Niño index for the past 200 years, Moy et al. have demonstrated that only moderate-to-strong El Niño events are archived in the lake sediments. Nonetheless, no quantitative or semi-quantitative record of ENSO intensity is presently available for the Holocene.

(h) *Abiyata lake-level record*. To characterize the EM we used the Abiyata lake-level record (Chalié and Gasse, 2002) based on diatom-inferred conductivity values expressed in log μS cm^{-1}. Standard errors are 0.35 for conductivity (log).

3. Results and discussion

3.1. ITCZ pacing of Nile delta morphogenesis

To infer changes in the water balance of the Nile basin at millennial timescales, we produced a spatially averaged time-series of Holocene sedimentation rates for the delta area (Fig. 5a). The most recent figures of 160 mm $century^{-1}$ fit tightly with pre-1964 measurements of deltaic accretion (Shahin, 1985) and corroborate the robustness of our record. Sedimentation rates span a range of ~220 mm $century^{-1}$ and document two distinct features. First, the onset of deltaic deposition ~8500 years ago linked to the drowning of the Pleistocene floodplain by rising Holocene sea levels. Second, a gradual long-term decrease in sediment loadings is recorded from a maximum of 355 mm $century^{-1}$ at ~7700 cal. BP to a minimum of 138 mm $century^{-1}$ at ~1200 cal. BP. This time-series displays remarkable similarities with a number of northern tropics precipitation archives, namely the Qunf (Fleitmann et al., 2003) (Oman, $r^2 = 0.77$, $P < 0.0001$; $Lag_0 = -0.88$; Fig. 5d) and Dongge (Wang et al., 2005) Cave stalagmites (southern China, $r^2 = 0.8$, $P < 0.0001$; $Lag_0 = -0.9$; Fig. 5e), and the Cariaco Basin (Haug et al., 2001) marine sediments (Venezuela, $r^2 = 0.73$, $P < 0.0001$; $Lag_0 = 0.86$; Figs. 5f and 8). These relationships demonstrate that the Nile's hydro-system has responded to a gradual precession-driven shift in the mean boreal position of the ITCZ (insolation 30°N: $r^2 = 0.87$, $P < 0.0001$, $Lag_0 = -0.93$; Williams et al., 2000, 2006, 2010; Williams, 2009). A time-progressive decrease in summer insolation reduced Africa's land/sea contrast and therefore the northern movement of monsoonal rainfall belts, which, for the Nile valley, lay ~500 km north of present during the early Holocene (Gasse, 2000). Convective activity within the ITCZ was furthermore reduced by a gradual decrease in monsoon wind strength over East Africa, and therefore moisture influx from the southern Indian Ocean (Bassinot et al., 2011).

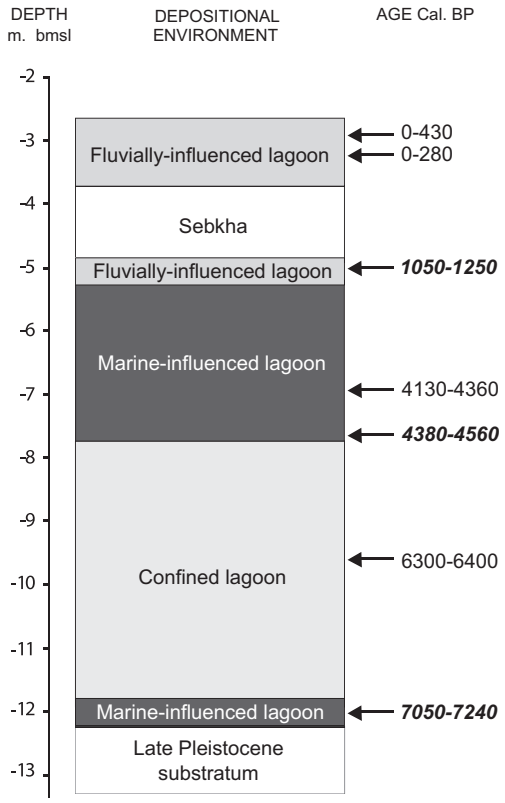

Fig. 4. Type stratigraphy of the Maryut basin showing the timing and nature of change dates (denoted in bold italics). For details see Flaux (2012).

The termination of mid-Holocene humid conditions in North Africa appears to be spatially and temporally contrasted (deMenocal et al., 2000; Kröpelin et al., 2008). In Egypt and Sudan, intensification of arid conditions probably reached a threshold ~5500 cal. BP, after which point pastoral activities beyond the Nile valley were no longer sustainable (Kuper and Kröpelin, 2006). This tipping point is translated by a step-like decrease in occupation sites (Fig. 5b) concomitant with a depopulation of the Sahara's eastern savannah driven by increasingly inhospitable climate conditions. By ~5500 cal. BP full desert conditions are already evident in southern Egypt and Sudan (Woodward et al., 2001; Nicoll, 2004) and a number of the Nile's upper-reach tributaries had stopped flowing. Around 5500 cal. BP Wadi el Melik was desiccated (Pachur and Hoelzmann, 1991) and flow from Wadi Howar, the southern tributary of the Nile in Sudan, ebbed significantly (Pachur and Kröpelin, 1987). We record a discernable ~15% increase in Nile sedimentation rates between ~5500 and 4800 cal. BP, a sediment pulse that could be consistent with vegetation dieback in the Nile valley and eastern desert. Dust production linked to arid conditions in the Sahara further accentuated drier conditions by reducing monsoonal rainfall via a direct cooling of the surface (Ganopolski et al., 1998; Mulitza et al., 2010). These precession-driven changes in climate dynamics participated in the concentration of societies along the Nile's fluvial corridor, and acted as a precursor to the emergence of its first politically centralized civilizations (Butzer, 1976; Hassan, 1997; Brooks, 2006, 2011; Kuper and Kröpelin, 2006).

3.2. Sub-millennial ENSO-like modulation of Nile delta changes

We constructed a second record using radiocarbon Probability Density Functions (PDF), to explore Holocene catchment-scale changes and deltaic morphogenesis at sub-millennial timescales (Fig. 7). This time-series illustrates that secular changes in Nile hydrology are superimposed on the first-order precession-driven trend. One major climatic forcing of Holocene climate variability at sub-millennial timescales resides in solar activity (Knudsen, 2009). Changes in solar activity have notably had important repercussions on northern hemisphere temperatures and the mean position of the ITCZ, that intimately responds to North Atlantic climate (Wang et al., 2005). Nonetheless, we find that neither the North Atlantic Bond events (Bond et al., 2001) nor variability in the high-resolution monsoon records of Arabia (Fleitmann et al., 2003) and southern Asia (Wang et al., 2005) satisfactorily explain the sub-millennial changes in our Nile PDF data.

Another mechanism may involve interactions between Holocene solar activity and ENSO (Emile-Geay et al., 2007). Instrumental records demonstrate that, over large parts of Africa, ENSO-like processes are important drivers of decadal variations in precipitation (Indeje et al., 2000; Nicholson and Selato, 2000). Analysis of modern instrumental records shows a statistically significant relationship between the flooding regime of the Nile and ENSO-indices (Wang and Eltahir, 1999; Ortlieb, 2004; Williams and Nottage, 2006), principally with regards to the hydrology of the Blue Nile and Atabara that presently contribute 68% and 22% of peak flow and 61% and 25% of the Nile's annual suspended load (Garzanti et al., 2006; Williams, 2009). Krom et al. (2002) suggest that the Blue Nile, mantled in the erodible Tertiary volcanic rocks of the Ethiopian highlands, has been the dominant catchment in modulating source to sink sediment fluxes for at least the past 5000 years (Revel et al., 2010; Padoan et al., 2011). To assess whether ENSO-like frequency (Moy et al., 2002) was a significant driver of sub-millennial shifts in our Nile record, we used Cross-Correlation Analysis (CCA) ($P = 0.05$).

3.2.1. 7000 to 4600 cal. BP

The strength of the CCA ($Lag_0 = +0.71$) for the period 7000–4600 cal. BP underlines a strong coupling between the Nile PDF record and high ENSO-like variance (Moy et al., 2002). The Nile-ENSO correlation for this phase was further confirmed using a three-step multivariate cluster analysis, principal components analysis and non-metric multidimensional scaling (Figs. 8 and 9). We suggest that intensification of interannual oscillations between dry El Niño years versus cold-phase La Niña floods and a more intense Ethiopian Monsoon (Tierney et al., 2011) controlled erosion and discharge, particularly in the Blue Nile catchment, mediating widespread changes in the base-level depocentre. Present data demonstrate that increased rains in the Sahelian–Sudanian belt are related to stronger W–SW low-level winds and an East Tropical Jet close to 200 hPa (Camberlin, 2009). Cold La Niña episodes are generally accompanied by anomalous northerly ITCZ shifts and intense monsoons, while the opposite is true of warm El Niño years (Joly and Voldoire, 2009). The high CCA values suggest that ENSO-related changes in monsoon strength operated during this time period, as prominent sub-millenial scale ENSO changes have recently been identified in the tropical Pacific (Marchitto et al., 2010). Such a relationship between ENSO-like frequency and East African precipitation would have been amplified during the so-called 'African Humid Phase', when the mean summer ITCZ extended over northern Sudan and southern Egypt. This scenario is supported by the PMIP2 mid-Holocene modelling experiment showing a stronger summer Ethiopian Monsoon, driven by sharper northern hemisphere seasonality and enhanced continental-ocean temperature gradients (Braconnot et al., 2007) (Fig. 5h).

3.2.2. 4600 to 2500 cal. BP

A decoupling of the Nile and ENSO time-series between 4600 and 2500 cal. BP (correlation $Lag_0 = -0.22$; Fig. 3) is consistent with

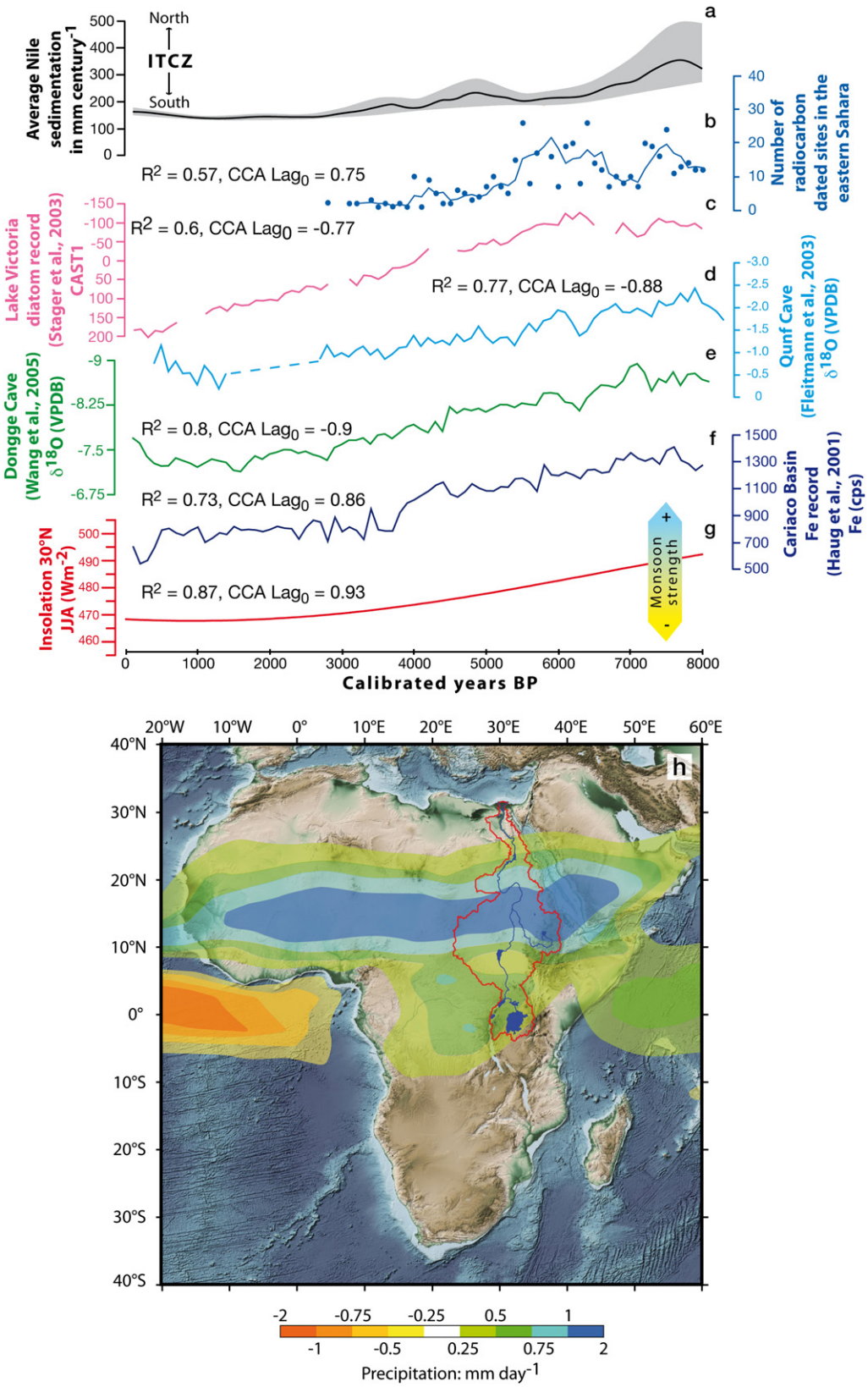

Fig. 5. Comparison of Nile delta sedimentation with eastern Sahara archaeological and northern tropics palaeoclimate records. (a) Spatially averaged Nile delta sedimentation record (this study; light grey envelope denotes minimum and maximum sedimentation rates), plotted alongside (b) evolution of radiocarbon dated sites in Egypt and Sudan's eastern desert (solid line denotes three-point moving average); (c) Lake Victoria diatom record (Stager et al., 2003) (CAST1 = Correspondence Analysis, Square root Transformed); (d) the Qunf Cave (Fleitmann et al., 2003), and (e) Dongge Cave (Wang et al., 2005) stalagmite records, (f) the Cariaco Basin Fe record (Haug et al., 2001) and (g) insolation curve at 30°N, averaged from June to August. (h) June–July–August–September mean precipitation differences (mm day^{-1}) between Mid-Holocene (6000 cal. BP) and preindustrial for the mean of PMIP2 simulations (Braconnot et al., 2007). The Nile catchment is denoted by the red line. Statistical relationships with the Nile sediment record are given. (For interpretation of the references to colour in this figure legend, the reader is referred to the web version of this article.)

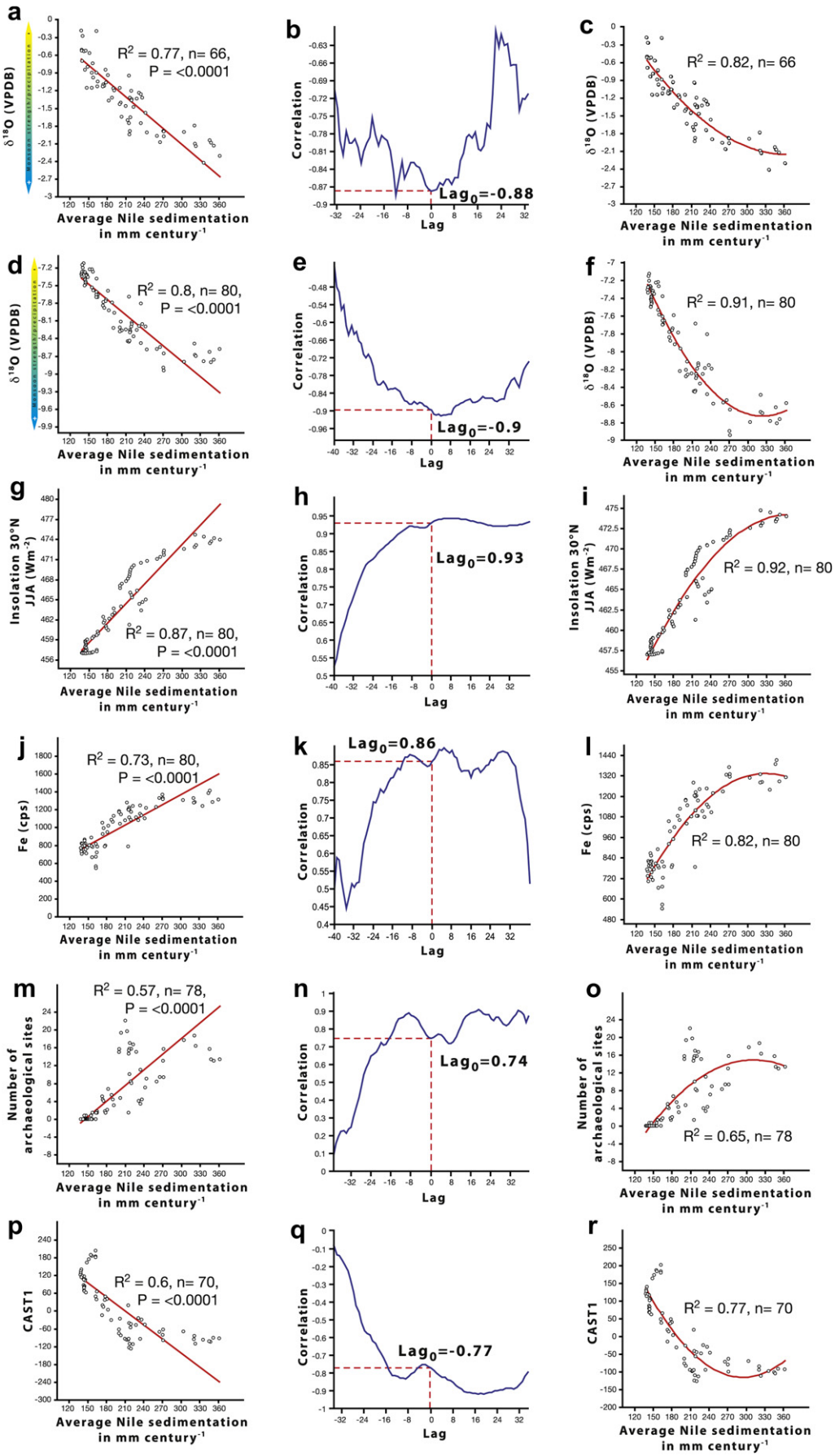

Fig. 6. Linear, CCA and polynomial (second order) statistical analyses of Nile sedimentation rates (mm century^{-1}) versus (a–c) Qunf (Fleitmann et al., 2003); (d–f) Dongge (Wang et al., 2005); (g–i) insolation 30°N (Laskar et al., 2004); (j–l) the Cariaco Basin (Haug et al., 2001); (m–o) the number of archaeological sites in Egypt and Sudan's eastern desert; (p–r) Lake Victoria diatom record (Stager et al., 2003).

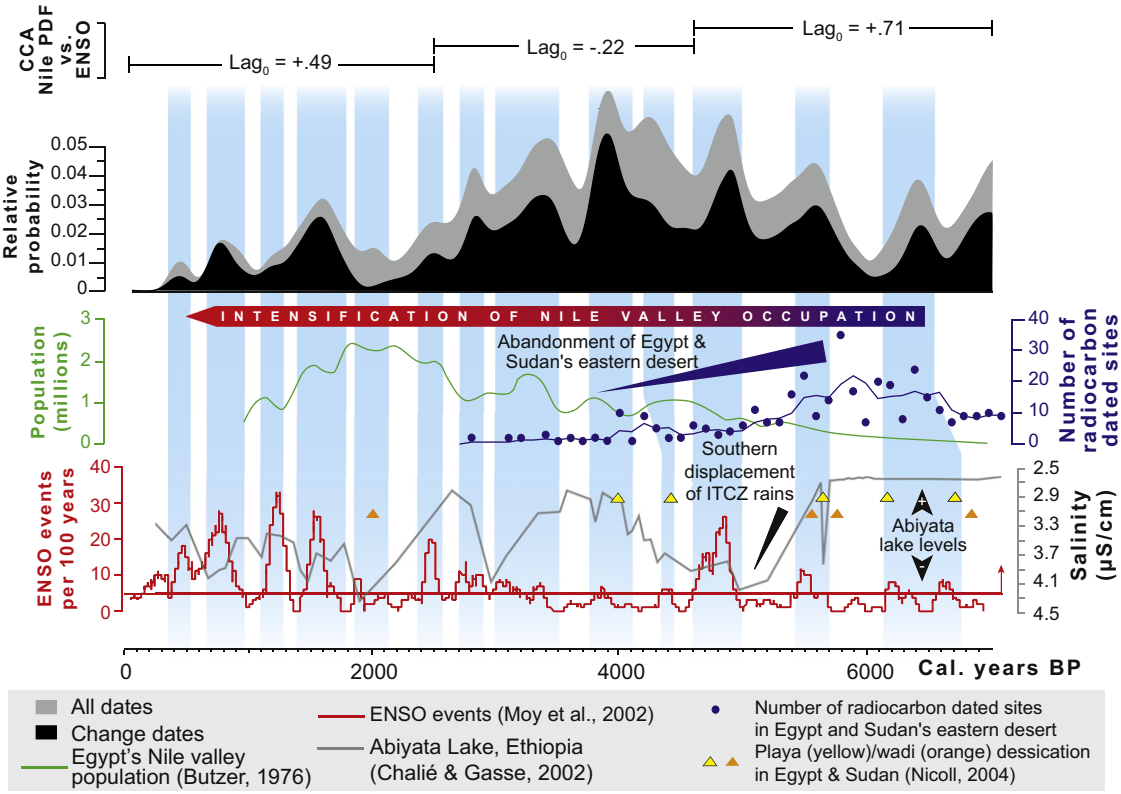

Fig. 7. Time-series of Nile PDFs from 7000 cal. BP to present. PDFs are depicted alongside radiocarbon dated archaeological sites in Egypt and Sudan's eastern desert (solid blue line denotes three-point moving average, Kuper and Kröpelin, 2006), Egypt's Nile valley population (Butzer, 1976), the number of ENSO events per 100 years (Moy et al., 2002), Abiyata (Ethiopia) lake levels (Chalié and Gasse, 2002), and playa and wadi desiccation (Nicoll, 2004). (For interpretation of the references to colour in this figure legend, the reader is referred to the web version of this article.)

(i) a southern shift in the mean summer position of the ITCZ (Fig. 1b), which may have reduced the interactions between ENSO-like frequency and the Ethiopian Monsoon; and (ii) a decrease in ENSO-like frequency (Moy et al., 2002). It appears that during this phase, non-ENSO climatic factors provided the main pacemaker for fluvial sedimentation. Furthermore, Stanley and Warne (1993) have identified a change in the deltaic regime during this phase characterized by a shift from a 'fluvial-dominated cuspate delta' to a 'wave-dominated arcuate delta' which might have partially masked the archiving of a weakened ENSO signal in the deltaic sediments.

This period also corresponds to the onset of marked human activities in the Nile valley. The 4600 cal. BP transition is closely correlated with both historical and radiocarbon chronologies for the beginning of the Egyptian Old Kingdom and the first regnal year of Pharaoh Djoser at 4617 BP (Shaw, 2000), 4542 BP (Hornung et al., 2006), or 4593–4626 cal. BP (Bronk-Ramsey et al., 2010). Intensification of human occupation throughout the Nile valley came in response to regional desertification (Kuper and Kröpelin, 2006). Nomadic populations that had previously practiced seasonal migration between the Nile valley and the Saharan savannah settled along the banks of the Nile in response to failing summer precipitation and the desiccation of rain-fed playas and wadis (Nicoll, 2001, 2004). The success of ancient Nile valley civilizations stemmed partly from their ability to adapt to the changing conditions of the Nile (Butzer, 1976; Hassan, 1997; Welsby, 2001; Welsby et al., 2002) and we suggest that reduced river flow linked to a weakening of the Ethiopian Monsoon was particularly conducive to the expansion of agriculture by: (i) exposing productive floodplain lands for cultivation; and (ii) producing a sharper contrast between seasonally-driven Nile minima and maxima. Williams (2009) has also suggested that this aridity might have enhanced river incision and the drainage of previously swampy land in proximity to the main Nile channel.

The predictable flooding and controlled irrigation of the fertile valley generated surplus crops, which in turn promoted social development and culture (Butzer, 1976). By ~4600 years ago, Egyptian and Nubian civilizations were heavily dependent on Nile hydrology, expressed by a transition to artificial irrigation around the end of the Predynastic period (Hassan, 1997). The first recorded evidence of water management in the Nile valley derives from a mace-head of the King Scorpion, the last of the Predynastic kings (Butzer, 1976). Further examples include the Sadd-el-Kafara dam constructed ~2600–2700 BC (Mays, 2010) and the Hawara Channel cleared to drain floodwaters from the Nile into the Faiyum basin during the reign of Khakheperra Senusret II (1877–1870 BC) (Shaw, 2000). The Nile delta also underwent significant shifts in its sediment supply during this period. Our spatially averaged sedimentation record shows a two-step decrease in flood-driven accretion ~4400–4100 cal. BP (−25%) and ~3700–3100 cal. BP (−25%) (Fig. 5a). These episodes of decreased Nile delta sediment loading are in phase with other regional palaeoclimate archives (Chalié and Gasse, 2002; Thompson et al., 2002), including the desiccation of Nile-fed Lake Faiyum ~4200 cal. BP (Hassan, 1997). Such evidence suggests that the end of Egypt's Old Kingdom ~4200 cal. BP was partly forced by regional aridification and the failure of Nile floods. For instance, an important inscription on the tomb of Ankhtifi, a nomarch during the early First Intermediate Period, describes the great famines that crippled the land ~4200–4050 cal. BP (Shaw, 2000). Climatic changes, in association with the historical and anthropological contexts, therefore appear critical in explaining the waxing and waning of Nile civilizations.

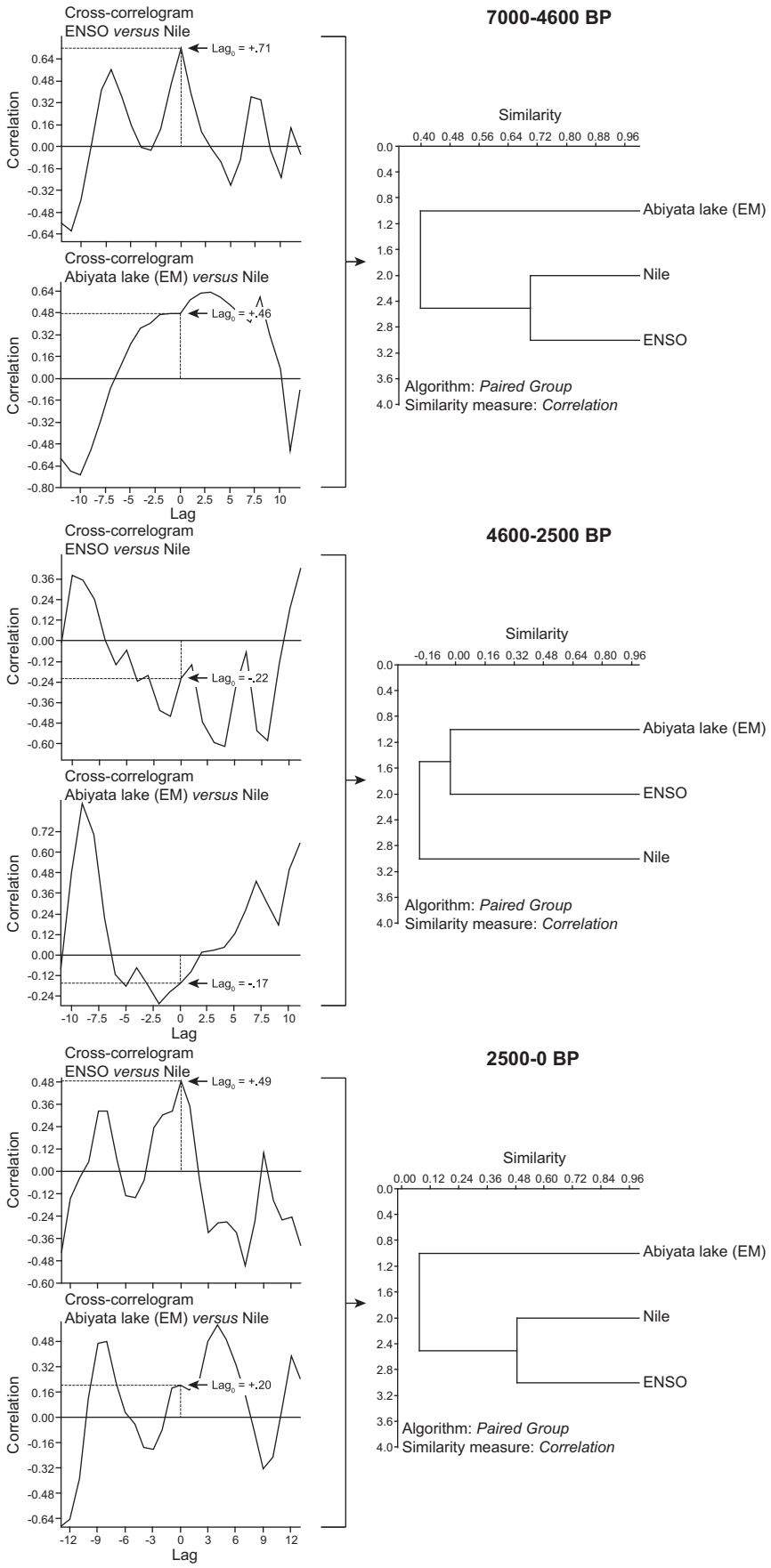

Fig. 8. CCA of Nile versus ENSO and Abiyata lake-level (EM) time-series ($P = 0.05$).

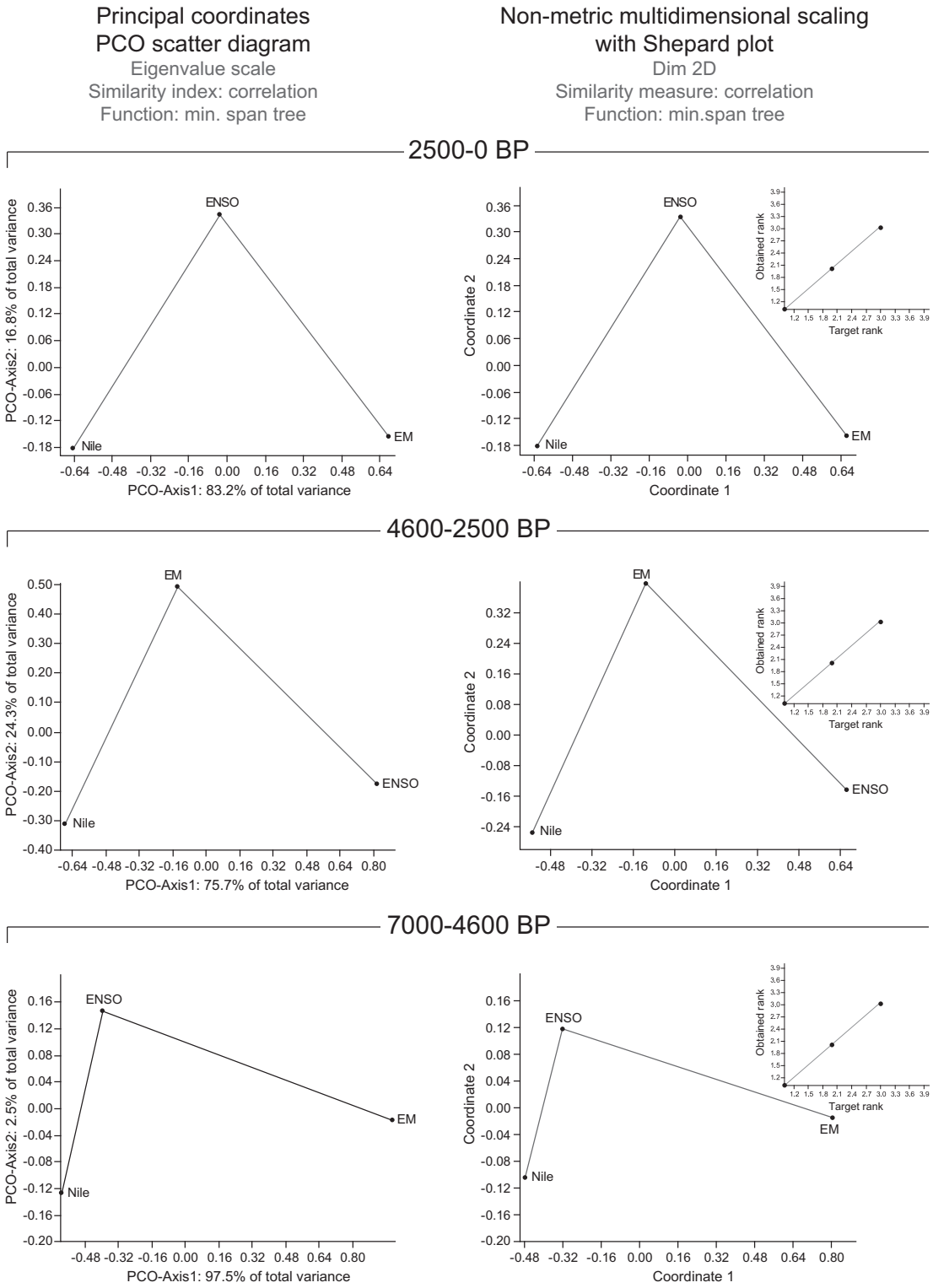

Fig. 9. Ordination of Nile, ENSO and Abiyata lake (EM) time-series using principal coordinates, and non-metric multidimensional scaling (with Shepard plot) for the three periods (7000–4600, 4600–2500 and 2500–0 BP). The min span tree function, linking proximal variances, was always used. The period 7000–4600 BP shows the closest numerical distribution of Nile and ENSO time-series whereas the 4600–2500 BP time range corresponds to the highest difference. The 2500–0 BP period orders a median distribution of the ENSO time-series.

3.2.3. 2500 cal. BP to present

Between 2500 cal. BP and present, a significant CCA ($Lag_0 = +0.49$) for the Nile versus ENSO time-series demonstrates that a renewed intensification in ENSO-like frequency was one of the key pacemakers of deltaic change. This interval corresponds to much higher centennial-scale ENSO-like frequency (up to 31 events century^{-1}) compared to <10 century^{-1} for the preceding period 4600–2500 cal. BP (Moy et al., 2002). Transient oscillations

between El Niño aridity and La Niña flooding significantly impacted upon the Nile valley's geosystems. Weakening of the CCA compared to the early Holocene is attributed to a more southerly ITCZ (mean summer maximum ~15°N), increasing the proportion of sub-equatorial rains over the White Nile to the detriment of the Blue Nile catchment.

On the delta, important irrigation systems (e.g. canal Damanhur, Shabour, Shanasha) were put into place during this period, modifying water and sediment transport pathways. Lift irrigation coupled with a well-structured entrepreneurial system allowed agriculture to expand and intensify from Ptolemaic times onwards (Shaw, 2000). In addition to traditional flood crops, spread of the waterwheel spawned the introduction of summer harvests and, with it, an intensification of human exploitation of the deltaic plain. By Roman times, the Nile delta constituted one of the Mediterranean's most important grain-producing regions.

4. Conclusion

These high-resolution Nile records demonstrate that deltas are key base-level archives to understand the interplay between climate forcings and human occupation (Nicoll, 2004; Brooks, 2006, 2011). During the past ~8000 years, the Nile's catchment-scale changes have been modulated by a first-order weakening of the Ethiopian Monsoon's intensity driven by a millennial-scale southern displacement of the ITCZ, whilst on sub-millennial timescales, the temporal pattern of deltaic change bears ENSO-like signatures. Transient El Niño-La Niña oscillation cycles during periods of high ENSO activity pulsed water-flow and sediment delivery to the delta area, acting as one of the chief drivers of geomorphological change at the regional scale. The hydro-geomorphological signatures of these global dynamics were locally exacerbated by an intensification of human occupation of the Nile valley (Kuper and Kröpelin, 2006), particularly from the Pharaonic period onwards. The integration and normalization of well-resolved chronostratigraphic datasets from other world deltas has a central role to play in furthering understanding of how continental-scale fluvial systems have responded to both Holocene global dynamics and societal impacts, as well as in providing useful templates for validating numerical models aimed at investigating the complexity of human–climate interactions (Gaillard et al., 2010).

Acknowledgements

We thank two anonymous referees, R. Bonnefille, M. Taieb and E. Van Campo for critical review and comments on earlier versions of the manuscript. Research was funded by ANR Paleomed (09-BLAN-0323-01), Artemis INSU, PEPS INSHS and PEPS INEE.

References

Bassinot, F.C., Marzin, C., Braconnot, P., Marti, O., Mathien-Blard, E., Lombard, F., Bopp, L., 2011. Holocene evolution of summer winds and marine productivity in the tropical Indian Ocean in response to insolation forcing: data-model comparison. Climate of the Past 7, 815–829.

Bond, G., Kromer, B., Beer, J., Muscheler, R., Evans, M.N., Showers, W., Hoffmann, S., Lotti-Bond, R., Hajdas, I., Bonani, G., 2001. Persistent solar influence on North Atlantic climate during the Holocene. Science 294, 2130–2136.

Braconnot, P., Otto-Bliesner, B., Harrison, S., Joussaume, S., Peterchmitt, J.-Y., Abe-Ouchi, A., Crucifix, M., Driesschaert, E., Fichefet, Th., Hewitt, C.D., Kageyama, M., Kitoh, A., Laîné, A., Loutre, M.-F., Marti, O., Merkel, U., Ramstein, G., Valdes, P., Weber, S.L., Yu, Y., Zhao, Y., 2007. Results of PMIP2 coupled simulations of the Mid-Holocene and Last Glacial Maximum – Part 1: experiments and large-scale features. Climate of the Past 3, 261–277.

Bronk Ramsey, C., 2000. OxCal Program v3.5: The Manual.

Bronk-Ramsey, C., Dee, M.W., Rowland, J.M., Higham, T.F., Harris, S.A., Brock, F., Quiles, A., Wild, E.M., Marcus, E.S., Shortland, A.J., 2010. Radiocarbon-based chronology for dynastic Egypt. Science 328, 1554–1557.

Brooks, N., 2006. Cultural responses to aridity in the Middle Holocene and increased social complexity. Quaternary International 151, 29–49.

Brooks, N., 2011. Human responses to climatically-driven landscape change and resource scarcity: learning from the past and planning for the future. In: Martini, I.P., Chesworth, W. (Eds.), Landscapes and Societies. Springer, pp. 43–66.

Bubenzer, O., Riemer, H., 2007. Holocene climatic change and human settlement between the Central Sahara and the Nile Valley: archaeological and geomorphological results. Geoarchaeology: An International Journal 22, 607–620.

Butzer, K.W., 1976. Early Hydraulic Civilization in Egypt: a Study in Cultural Ecology. University of Chicago Press, Chicago.

Butzer, K.W., 1997. Late Quaternary problems of the Egyptian Nile: stratigraphy, environments, prehistory. Paléorient 23, 151–173.

Camberlin, P., 2009. Nile basin climates. In: Dumont, H.J. (Ed.), The Nile: Origin, Environments, Limnology and Human Use. Springer, London, pp. 307–333.

Chalié, F., Gasse, F., 2002. Late-Glacial–Holocene diatom record of water chemistry and lake-level change from the tropical East African Rift Lake Abiyata (Ethiopa). Palaeogeography, Palaeoclimatology, Palaeoecology 187, 259–283.

deMenocal, P., Ortiz, J., Guilderson, T., Sarnthein, M., 2000. Coherent high- and low-latitude climate variability during the Holocene warm period. Science 288, 2198–2202.

Ducassou, E., Mulder, T., Migeon, S., Gonthier, E., Murat, A., Revel, M., Capotondi, L., Bernasconi, S.M., Mascle, J., Zaragosi, S., 2008. Nile floods recorded in deep Mediterranean sediments. Quaternary Research 70, 382–391.

Emile-Geay, J., Cane, M., Seager, R., Kaplan, A., Almasi, P., 2007. El Niño as a mediator of the solar influence on climate. Paleoceanography 22, PA3210.

Flaux, C., Morhange, C., Marriner, N., Rouchy, J.-M., 2011. Balance entre les influences marines et nilotiques dans le budget hydrologique de la lagune du Mariout (delta du Nil) entre 7800 et 3000 cal. BP. Géomorphologie 3, 261–278.

Flaux, C., 2012. Holocene palaeo-environments of the Maryut lagoon in the NW Nile delta, Egypt. PhD thesis, Université Aix-Marseille, Aix-en-Provence.

Fleitmann, D., Burns, S.J., Mudelsee, M., Neff, U.N., Kramers, J., Mangini, A., Matter, A., 2003. Holocene forcing of the Indian monsoon recorded in a stalagmite from Southern Oman. Science 300, 1737–1739.

Fleitmann, D., Burns, S.J., Mangini, A., Mudelsee, M., Kramers, J., Villa, I.M., Neff, U., Al-Subbary, A.A., Buettner, A., Hippler, D., Matter, A., 2007. Holocene ITCZ and Indian monsoon dynamics recorded in stalagmites from Oman and Yemen (Socotra). Quaternary Science Reviews 26, 170–188.

Gaillard, M.-J., Sugita, S., Mazier, F., Trondman, A.-K., Broström, A., Hickler, T., Kaplan, J.O., Kjellström, E., Kokfelt, U., Kuneš, P., Lemmen, C., Miller, P., Olofsson, J., Poska, A., Rundgren, M., Smith, B., Strandberg, G., Fyfe, R., Nielsen, A.B., Alenius, T., Balakauskas, L., Barnekow, L., Birks, H.J.B., Bjune, A., Björkman, L., Giesecke, T., Hjelle, K., Kalnina, L., Kangur, M., van der Knaap, W.O., Koff, T., Lagerâs, P., Latałowa, M., Leydet, M., Lechterbeck, J., Lindbladh, M., Odgaard, B., Peglar, S., Segerström, U., von Stedingk, H., Seppä, H., 2010. Holocene land-cover reconstructions for studies on land cover-climate feedbacks. Climate of the Past 6, 483–499.

Ganopolski, A., Kubatzki, C., Clausen, M., Brovkin, V., Petoukhov, V., 1998. The influence of vegetation-atmosphere-ocean on climate during the mid-Holocene. Science 280, 1916–1919.

Garzanti, E., Ando, S., Vezzoli, G., Megid, A.A., Kammar, A., 2006. Petrology of Nile River sands (Ethiopia and Sudan): sediment budgets and erosion patterns. Earth and Planetary Science Letters 252, 327–341.

Gasse, F., 2000. Hydrological changes in the African tropics since the Last Glacial Maximum. Quaternary Science Reviews 19, 189–211.

Hajiana, S., Sadegh Movahed, M., 2010. Multifractal detrended cross-correlation analysis of sunspot numbers and river flow fluctuations. Physica A: Statistical Mechanics and Its Applications 389, 4942–4957.

Hassan, F.A., 1997. The dynamics of a riverine civilization: a geoarchaeological perspective on the Nile Valley, Egypt. World Archaeology 29, 51–74.

Haug, G.H., Hughen, K.A., Sigman, D.M., Peterson, L.C., Röhl, U., 2001. Southward migration of the intertropical convergence zone through the Holocene. Science 293, 1304–1308.

Hornung, E., Krauss, R., Warburton, D.A., 2006. Ancient Egyptian Chronology. Brill, Leiden.

Indeje, M., Semazzi, F.H.M., Ogallo, L.J., 2000. ENSO signals in East African rainfall seasons. International Journal of Climatology 20, 19–46.

Joly, M., Voldoire, A., 2009. Influence of ENSO on the West African monsoon: temporal aspects and atmospheric processes. Journal of Climate 22, 3193–3210.

Knudsen, M.F., 2009. Taking the pulse of the Sun during the Holocene by joint analysis of ^{14}C and ^{10}Be. Geophysical Research Letters 36, L16701.

Krom, M.D., Stanley, J.D., Cliff, R.A., Woodward, J.C., 2002. Nile river fluctuations over the past 7000 yrs and their key role in sapropel development. Geology 30, 71–74.

Kröpelin, S., Verschuren, D., Lézine, A.-M., Eggermont, H., Cocquyt, C., Francus, P., Cazet, J.-P., Fagot, M., Rumes, B., Russell, J.M., Darius, F., Conley, D.J., Schuster, M., von Suchodoletz, H., Engstrom, D.R., 2008. Climate-driven ecosystem succession in the Sahara: the past 6000 years. Science 320, 765–768.

Kuper, R., Kröpelin, S., 2006. Climate-controlled Holocene occupation of the Sahara: motor of Africa's evolution. Science 313, 803–807.

Laskar, J., Robutel, P., Joutel, F., Gastineau, M., Correia, A.C.M., Levrard, B., 2004. A long term numerical solution for the insolation quantities of the Earth. Astronomy and Astrophysics 428, 261–285.

Leduc, G., Vidal, L., Cartapanis, O., Bard, E., 2009. Modes of Eastern Equatorial Pacific thermocline variability: implications for ENSO dynamics over the last glacial period. Paleoceanography 24, PA3202. doi:10.1029/2008PA1701.

Macklin, M.G., Lewin, J., 2003. River sediments, great floods and centennial-scale Holocene climate change. Journal of Quaternary Science 18, 101–105.
Macklin, M.G., Benito, G., Gregory, K.J., Johnstone, E., Lewin, J., Michczynska, D.J., Soja, R., Starkel, L., Thorndycraft, V.R., 2006. Past hydrological events reflected in the Holocene fluvial record of Europe. Catena 66, 145–154.
Macklin, M., Jones, A.F., Lewin, J., 2010. River response to rapid Holocene environmental change: evidence and explanation in British catchments. Quaternary Science Reviews 29, 1555–1576.
Marchitto, T.M., Muscheler, R., Ortiz, J.D., Carriquiry, J.D., van Geen, A., 2010. Dynamical response of the tropical Pacific Ocean to solar forcing during the early Holocene. Science 330, 1378–1381.
Mays, L.W., 2010. Ancient Water Technologies. Springer, London.
Moy, C.M., Seltzer, G.O., Rodbell, D.T., Anderson, D.M., 2002. Variability of El Niño southern oscillation activity at millennial timescales during the Holocene epoch. Nature 420, 162–165.
Mulitza, S., Heslop, D., Pittauerova, D., Fischer, H.W., Meyer, I., Stuut, J.B., Zabe, M., Mollenhauser, G., Collins, J.A., Kuhnert, H., Schulz, M., 2010. Increase in African dust flux at the onset of commercial agriculture in the Sahel region. Nature 466, 226–228.
Nicholson, S.E., Selato, J.C., 2000. The influence of La Nina on African rainfall. International Journal of Climatology 20, 1761–1776.
Nicoll, K., 2001. Radiocarbon chronologies for prehistoric human occupation and hydroclimatic change, Egypt and Sudan. Geoarchaeology: An International Journal 16, 47–64.
Nicoll, K., 2004. Recent environmental change and prehistoric human activity in Egypt and Northern Sudan. Quaternary Science Reviews 23, 561–580.
Ortlieb, L., 2004. Historical chronology of ENSO and the Nile flood record. In: Battarbee, R.W., Gasse, F., Stickley, C.E. (Eds.), Past Climate Variability Through Europe and Africa. Springer, London, pp. 257–278.
Pachur, H.J., Hoelzmann, P., 1991. Palaeoclimatic implications of late Quaternary lacustrine sediments in western Nubia, Sudan. Quaternary Research 36, 257–276.
Pachur, H.J., Kröpelin, S., 1987. Wadi Howar: paleoclimatic evidence from an extinct river system in the southeastern Sahara. Science 237, 298–300.
Padoan, M., Garzanti, E., Harlavan, Y., Villa, I.M., 2011. Tracing Nile sediment sources by Sr and Nd isotope signatures (Uganda, Ethiopia, Sudan). Geochimica et Cosmochimica Acta 75, 3627–3644.
Podobnik, B., Stanley, H.E., 2008. Detrended cross-correlation analysis: a new method for analyzing two nonstationary time series. Physical Review Letters 100, 084102.
Reimer, P.J., Baillie, M.G.L., Bard, E., Bayliss, A., Beck, J.W., Blackwell, P.G., Bronk Ramsey, C., Buck, C.E., Burr, G.S., Edwards, R.L., Friedrich, M., Grootes, P.M., Guilderson, T.P., Hajdas, I., Heaton, T.J., Hogg, A.G., Hughen, K.A., Kaiser, K.F., Kromer, B., McCormac, F.G., Manning, S.W., Reimer, R.W., Richards, D.A., Southon, J.R., Talamo, S., Turney, C.S.M., van der Plicht, J., Weyhenmeye, C.E., 2009. IntCal09 and Marine09 radiocarbon age calibration curves, 0–50,000 years cal. BP. Radiocarbon 51, 1111–1150.
Revel, M., Ducassou, E., Grousset, F.E., Bernasconi, S.M., Migeon, S., Revillon, S., Mascle, J., Murat, A., Zaragosi, S., Bosch, D., 2010. 100,000 years of African monsoon variability recorded in sediments of the Nile next term margin. Quaternary Science Reviews 29, 1342–1362.
Roberts, N., Barker, P., 1993. Landscape stability and biogeomorphic response to past and future climatic shifts in intertropical Africa. In: Thomas, D.S.G., Allison, R.J. (Eds.), Landscape Sensitivity. John Wiley and Sons Ltd, Chichester, pp. 65–82.
Shahin, M., 1985. Hydrology of the Nile Basin. Elsevier, Amsterdam.
Shaw, I., 2000. The Oxford History of Ancient Egypt. Oxford University Press, Oxford.
Sneh, A., Weissbrod, T., Ehrlich, A., Horowitz, A., Moshkovitz, S., Rosenfeld, A., 1986. Holocene evolution of the northeastern corner of the Nile Delta. Quaternary Research 26, 194–206.
Stager, J.C., Cumming, B.F., Meeker, L.D., 2003. A 10,000-year high-resolution diatom record from Pilkington Bay, Lake Victoria, East Africa. Quaternary Research 59, 172–181.
Stanley, J.-D., Warne, A.G., 1993. Nile delta: recent geological evolution and human impact. Science 260, 628–634.
Stanley, J.-D., McRea Jr., J.E., Waldron, J.C., 1996. Nile Delta Drill Core and Sample Database for 1985–1994: Mediterranean Basin (MEDIBA) Program. Smithsonian Contributions to the Marine Sciences, No. 37: Washington.
Stanley, J.-D., Bernasconi, M.P., Jorstad, T.F., 2008. Pelusium, an ancient port fortress on Egypt's Nile delta coast: its evolving environmental setting from foundation to demise. Journal of Coastal Research 24, 2451–2462.
Staubwasser, M., Weiss, H., 2006. Holocene climate and cultural evolution in late prehistoric–early historic West Asia. Quaternary Research 66, 372–387.
Thompson, L.G., Mosley-Thompson, E., Davis, M.E., Henderson, K.A., Brecher, H.H., Zagorodnov, V.S., Mashiotta, T.A., Lin, P.-N., 2002. Kilimanjaro ice core records: evidence of Holocene climate change in tropical Africa. Science 298, 589–593.
Thorndycraft, V.R., Benito, G., 2006. The Holocene fluvial chronology of Spain: evidence from a newly compiled radiocarbon database. Quaternary Science Reviews 25, 223–234.
Tierney, J.E., Lewis, S.C., Cook, B.I., LeGrande, A.N., Schmidt, G.A., 2011. Holocene evolution of summer winds and marine productivity in the tropical Indian Ocean in response to insolation forcing: data-model comparison. Earth and Planetary Science Letters 307, 103–112.
Törnqvist, T.E., 1994. Middle and late Holocene avulsion history of the River Rhine (Rhine–Meuse delta, Netherlands). Geology 22, 711–714.
Turney, C.S.M., Hobbs, D., 2006. ENSO influence on Holocene Aboriginal populations in Queensland, Australia. Journal of Archaeological Science 33, 1744–1748.
Verschuren, D., Sinninghe Damsté, J.S., Moernaut, J., Kristen, I., Blaauw, M., Fagot, M., Haug, G.H., Challacea Project Members, 2009. Half-precessional dynamics of monsoon rainfall near the East African Equator. Nature 462, 637–641.
Wang, G., Eltahir, E.A.B., 1999. Use of ENSO information in medium- and long-range forecasting of the Nile floods. Journal of Climate 12, 1726–1737.
Wang, Y., Cheng, H., Edwards, R.L., He, Y., Kong, X., An, Z., Wu, J., Kelly, M.J., Dykoski, C.A., Li, X., 2005. The Holocene Asian monsoon: links to solar changes and North Atlantic climate. Science 388, 854–857.
Welsby, D.A., Macklin, M.G., Woodward, J.C., 2002. Human responses to Holocene environmental changes in the Northern Dongola reach of the Nile, Sudan. In: Friedman, R. (Ed.), Egypt and Nubia: Gifts of the Desert. The British Museum Press, London, pp. 28–38.
Welsby, D.A., 2001. Life on the Desert Edge. Seven Thousand Years of Settlement in the Northern Dongola Reach. Sudan. BAR, Archaeopress, Oxford.
Williams, M., Nottage, J., 2006. Impact of extreme rainfall in the central Sudan during 1999 as a partial analogue for reconstructing early Holocene prehistoric environments. Quaternary International 150, 82–94.
Williams, M.A.J., Adamson, D.A., Cock, B., McEvedy, R., 2000. Late Quaternary environments in the white Nile region, Sudan. Global and Planetary Change 26, 305–316.
Williams, M., Talbot, M., Aharon, P., Abdl Salaam, Y., Williams, F., Brendeland, K.I., 2006. Abrupt return of the summer monsoon 15,000 years ago: new supporting evidence from the lower White Nile valley and Lake Albert. Quaternary Science Reviews 25, 2651–2665.
Williams, M.A.J., Williams, F.M., Duller, G.A.T., Munro, R.N., El Tom, O.A.M., Barrows, T.T., Macklin, M., Woodward, J., Talbot, M.R., Haberlah, D., Fluin, J., 2010. Late Quaternary floods and droughts in the Nile Valley, Sudan: new evidence from optically stimulated luminescence and AMS radiocarbon dating. Quaternary Science Reviews 29, 1116–1137.
Williams, M.A.J., 2009. Late Pleistocene and Holocene environments in the Nile basin. Global and Planetary Change 69, 1–15.
Wolff, C., Haug, G.H., Timmermann, A., Sinninghe Damsté, J.S., Brauer, A., Sigman, D.M., Cane, M.A., Verschuren, D., 2011. Reduced interannual rainfall variability in East Africa during the last ice age. Science 333, 743–747.
Woodward, J.C., Macklin, M.G., Welsby, D., 2001. The Holocene fluvial sedimentary record and alluvial geoarchaeology in the Nile Valley of northern Sudan. In: Maddy, D., et al. (Eds.), River Basin Sediment Systems: Archives of Environmental Change, Rotterdam, pp. 327–355.
Woodward, J.C., Macklin, M.G., Krom, M.D., Williams, M.A.J., 2007. The Nile: evolution, Quaternary River environments and material fluxes. In: Gupta, A. (Ed.), Large Rivers: Geomorphology and Management. Wiley, Chichester, pp. 261–292.